Witnessing nonclassical correlations via a single-shot experiment on an ensemble of spins using nuclear magnetic resonance

Amandeep Singh,[*] Arvind,[†] and Kavita Dorai[‡]
Department of Physical Sciences, Indian Institute of Science Education and Research Mohali, Sector 81 SAS Nagar, Manauli PO 140306 Punjab, India
(Received 8 January 2017; published 12 June 2017)

A bipartite quantum system in a mixed state can exhibit nonclassical correlations which can go beyond quantum entanglement. While quantum discord is the standard measure of quantifying such general quantum correlations, the nonclassicality can be determined by simpler means via the measurement of witness operators. We experimentally construct a positive map to witness nonclassicality of two qubits in an NMR system. The map can be decomposed in terms of measurable spin magnetizations so that a single run of an experiment on an ensemble of spins suffices to detect the nonclassicality in the state, if present. We let the state evolve in time and use the map to detect nonclassicality as a function of time. To evaluate the efficacy of the witness operator as a means to detect nonclassicality, we measure quantum discord by performing full quantum-state tomography at each time instant and obtain a fairly good match between the two methods.

DOI: 10.1103/PhysRevA.95.062318

I. INTRODUCTION

Quantum correlations are those correlations which are not present in classical systems, and in bipartite quantum systems are associated with the presence of quantum discord [1–3]. Such correlations in a bipartite mixed state can go beyond quantum entanglement and therefore can be present even if the state is separable [4]. The threshold between classical and quantum correlations was investigated in linear-optical systems by observing the emergence of quantum discord [5]. Quantum discord was experimentally measured in systems such as NMR that are described by a deviation density matrix [6–8]. Further, environment-induced sudden transitions in quantum discord dynamics and their preservation were investigated using NMR [9,10].

It has been shown that even with very low (or no) entanglement, quantum information processing (QIP) can still be performed using nonclassical correlations [11,12], which are typically characterized by the presence of quantum discord. However, computing and measuring quantum discord typically involves complicated numerical optimization, and furthermore, it has been shown that computing quantum discord is nondeterministic polynomial time-hard (NP) [13–15]. It is hence of prime interest to find other means, such as witnesses, to detect the presence of quantum correlations [16]. While there have been several experimental implementations of entanglement witnesses [17–19], there have been fewer proposals to witness nonclassicality. A nonlinear classicality witness was constructed for a class of two-qubit systems [20] and experimentally implemented using NMR [21,22], and was estimated in a linear optics system via statistics from a single measurement [23]. It is to be noted that as the state space for classical correlated systems is not convex, a witness for nonclassicality is more complicated to construct than a witness for entanglement and is necessarily nonlinear [24].

In this work we use two qubits to report the experimental detection of nonclassicality through a recently proposed positive map method [25]. Two NMR qubits have been recently used to demonstrate very interesting QIP phenomena, such as the quantum simulation of the ground state of a molecular Hamiltonian [26], the quantum simulation of the Avian compass [27], observing time-invariant coherences at room temperature [28], and preserving quantum discord [29]. The map is able to witness nonclassical correlations, going beyond entanglement, in a mixed state of a bipartite quantum system. The method requires much fewer experimental resources as compared to measurement of discord using full state tomography and therefore is an attractive alternative to demonstrating the nonclassicality of a separable state. The map implementation involves two-qubit gates and single-qubit magnetization measurements and can be achieved in a single experimental run using NMR. Our implementation of the nonclassicality witness involves the sequential measurement of different free induction decays (FIDs, corresponding to the NMR signal) in a single run of the same experiment. This is possible since NMR measurements are nondestructive, thus allowing sequential measurements on the same ensemble. We exploit this feature to implement the single-shot measurement of the map value. We perform experiments on a two-qubit separable state (nonentangled) which contains nonclassical correlations. Further, the state was allowed to freely evolve in time under natural NMR decohering channels, and the amount of nonclassicality present was evaluated at each time instant by calculating the map value. We compared our results using the positive map witness with those obtained by computing the quantum discord via full state tomography and obtained a good match.

However, beyond a certain time, the map was not able to detect nonclassicality, although the quantum discord measure indicated that nonclassicality was present in the state. This implies that while the positive map nonclassicality witness is easy to implement experimentally in a single experiment and

[*]amandeepsingh@iisermohali.ac.in
[†]arvind@iisermohali.ac.in
[‡]kavita@iisermohali.ac.in

is a good indicator of nonclassicality in a separable state, it is not able to characterize nonclassicality completely. In our case this is typified by the presence of a small amount of quantum discord when the state has almost decohered or when the amount of nonclassicality present is small. This, of course, leaves open the possibility of constructing a more optimal witness.

The material in this paper is organized as follows: Section II A contains a brief description of the construction of the positive map to detect nonclassicality, followed by details of the experimental NMR implementation in Sec. II B. The map value dynamics with time is contained in Sec. II C, while the comparison of the results of the positive map method with those obtained by measuring quantum discord via full quantum-state tomography is described in Sec. II D. Section III contains some concluding remarks.

II. EXPERIMENTALLY DETECTING NONCLASSICAL CORRELATIONS

A. Constructing the nonclassicality witness map

For pure quantum states of a bipartite quantum system which are represented by one-dimensional projectors $|\psi\rangle\langle\psi|$ in a tensor projector Hilbert space $\mathcal{H}_A \otimes \mathcal{H}_B$, the only type of quantum correlation is entanglement [30,31]. However, for mixed states the situation is more complex and quantum correlations can be present even if the state is separable, i.e., it is a classical mixture of separable pure states given by

$$\rho_{\text{sep}} = \sum_i w_i \rho_i^A \otimes \rho_i^B, \tag{1}$$

where w_i are positive weights and ρ_i^A, ρ_i^B are pure states in Hilbert spaces $\mathcal{H}_A$ and $\mathcal{H}_B$, respectively [32]. A separable state is called a properly classically correlated state (PCC) if it can be written in the form [33]

$$\rho_{\text{PCC}} = \sum_{i,j} p_{ij} |e_i\rangle^A\langle e_i| \otimes |e_j\rangle^B\langle e_j|, \tag{2}$$

where p_{ij} is a joint probability distribution, and $|e_i\rangle^A$ and $|e_j\rangle^B$ are local orthogonal eigenbases in local spaces $\mathcal{H}_A$ and $\mathcal{H}_B$, respectively. A state that cannot be written in the form given by Eq. (2) is called a nonclassically correlated (NCC) state. An NCC state can be entangled or separable.

The correlations in NCC states can go beyond those present in PCC states and are due to the fact that the eigenbases for the subsystems may not be orthogonal, i.e., the basis vectors are in a superposition [34]. A typical example of a bipartite two-qubit NCC state has been discussed in Ref. [35] and is given by

$$\sigma = \tfrac{1}{2}[|00\rangle\langle 00| + |1+\rangle\langle 1+|], \tag{3}$$

with $|+\rangle = \frac{1}{\sqrt{2}}(|0\rangle + |1\rangle)$. In this case the state has no product eigenbasis as the eigenbasis for subsystem B, since $|0\rangle$ and $|+\rangle$ are not orthogonal to each other. The state is separable (not entangled), as it can be written in the form given by Eq. (1); however, since it is an NCC state, it has nontrivial quantum correlations and has nonzero quantum discord. How to pin down the nonclassical nature of such a state with minimal experimental effort and without actually computing quantum discord is something that is desirable. It has been shown that such nonclassicality witnesses can be constructed using a positive map [25].

The map $\mathcal{W}$ over the state space $\mathcal{H} = \mathcal{H}_A \otimes \mathcal{H}_B$ takes a state to a real number $\mathbb{R}$:

$$\mathcal{W} : \mathcal{H} \longrightarrow \mathbb{R}. \tag{4}$$

This map is a nonclassicality witness map, i.e., it is capable of detecting NCC states in $\mathcal{H}$ state space if and only if [25]:

(a) for every bipartite state ρ_{PCC} having a product eigenbasis, $\mathcal{W}(\rho_{\text{PCC}}) \geqslant 0$;

(b) there exists at least one bipartite state ρ_{NCC} (having no product eigenbasis) such that $\mathcal{W}(\rho_{\text{NCC}}) < 0$.

A specific nonlinear nonclassicality witness map proposed by [25] is defined in terms of expectation values of positive Hermitian operators $\hat{A}_1, \hat{A}_2 \ldots \hat{A}_m$:

$$\mathcal{W}(\rho) = c - [\text{Tr}(\rho\hat{A}_1)][\text{Tr}(\rho\hat{A}_2)]\ldots[\text{Tr}(\rho\hat{A}_m)], \tag{5}$$

where $c \geqslant 0$ is a real number.

For the case of two-qubit systems using the operators $A_1 = |00\rangle\langle 00|$ and $A_2 = |1+\rangle\langle 1+|$ we obtain a nonclassicality witness map for the state in Eq. (3) as

$$\mathcal{W}_\sigma(\rho) = c - [\text{Tr}(\rho|00\rangle\langle 00|)][\text{Tr}(\rho|1+\rangle\langle 1+|)]. \tag{6}$$

The value of the constant c in the above witness map has to be optimized such that for any PCC state ρ having a product eigenbasis, the condition $\mathcal{W}_\sigma(\rho) \geqslant 0$ holds and the numerically optimized value of c as calculated in Ref. [25] is $c_{\text{opt}} = 0.182\,138\ldots$. The map given by Eq. (6) does indeed witness the nonclassical nature of the state σ as $[\text{Tr}(\rho|00\rangle\langle 00|)][\text{Tr}(\rho|1+\rangle\langle 1+|)]$ for $\rho \equiv \sigma$ has the value 0.25, which suggests that the state σ is an NCC state [25]. The value of a nonclassicality map, which when negative implicates the nonclassical nature of the state, is defined as its map value (MV).

B. NMR experimental system

We implemented the nonclassicality witness map $\mathcal{W}_\sigma$ on an NMR sample of ^{13}C-enriched chloroform dissolved in acetone-D6; the ^{1}H and ^{13}C nuclear spins were used to encode the two qubits (see Fig. 1 for experimental parameters). Unitary operations were implemented by specially crafted transverse radio frequency pulses of suitable amplitude, phase, and duration. Since a heteronuclear ^{1}H-^{13}C spin system was used to encode the qubits, standard pulse calibration methods available on the dedicated NMR spectrometer software were used for pulse optimization and gave accurate results. A sequence of spin-selective pulses interspersed with tailored free evolution periods were used to prepare the system in an NCC state as described below, written using spin-angular momentum operators:

$$\begin{aligned} I_{1z} + I_{2z} &\xrightarrow{(\pi/2)_x^1} -I_{1y} + I_{2z} \xrightarrow{Sp.Av.} I_{2z} \xrightarrow{(\pi/2)_y^2} I_{2x} \\ &\xrightarrow{\frac{1}{4J}} \frac{I_{2x} + 2I_{1z}I_{2y}}{\sqrt{2}} \xrightarrow{(\pi/2)_x^2} \frac{I_{2x} + 2I_{1z}I_{2z}}{\sqrt{2}} \\ &\xrightarrow{(-\pi/4)_y^2} \frac{(I_{2z} + I_{2x} + 2I_{1z}I_{2z} - 2I_{1z}I_{2x})}{2}. \end{aligned}$$

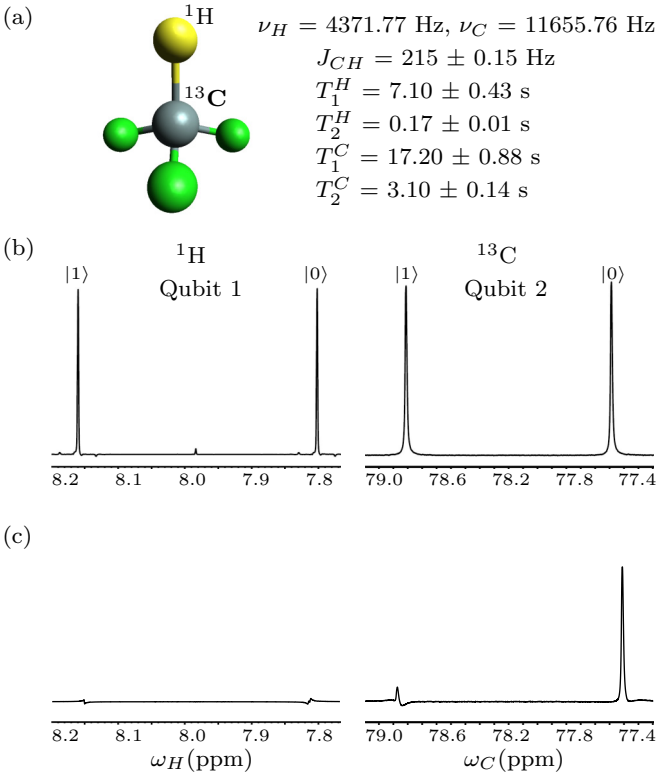

FIG. 1. (a) Pictorial representation of ^{13}C labeled chloroform with the two qubits encoded as nuclear spins of ^{1}H and ^{13}C; system parameters including chemical shifts ν_i, scalar coupling strength J (in Hz), and relaxation times T_1 and T_2 (in seconds) are tabulated alongside. (b) Thermal equilibrium NMR spectra of ^{1}H (Qubit 1) and ^{13}C (Qubit 2) after a $\frac{\pi}{2}$ readout pulse. (c) NMR spectra of ^{1}H and ^{13}C for the σ NCC state. Each transition in the spectra is labeled with the logical state ($|0\rangle$ or $|1\rangle$) of the "passive qubit" (not undergoing any transition).

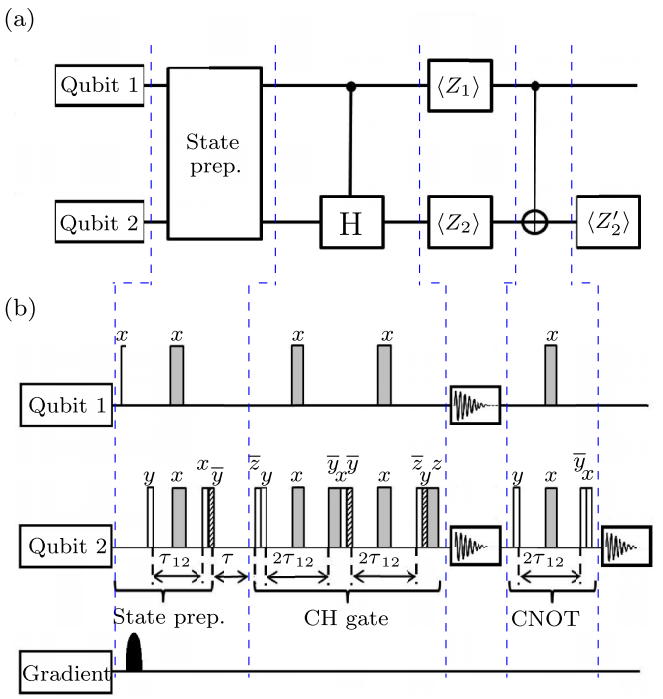

FIG. 2. (a) Quantum circuit and (b) NMR pulse sequence to create and detect an NCC state. Unfilled rectangles depict $\frac{\pi}{2}$ pulses, gray-shaded rectangles depict π pulses, and filled rectangles depict $\frac{\pi}{4}$ pulses, respectively. Phases are written above each pulse, with a bar over a phase indicating a negative phase. The evolution period was set to $\tau_{12} = \frac{1}{4J}$. The delay τ is the time for which the NCC state is allowed to evolve before detection, and the group of pulses and delays labeled as CH gate implement a controlled-Hadamard operation. The measurements of $\langle Z_1\rangle$, $\langle Z_2\rangle$, and $\langle Z_2'\rangle$ magnetizations in the circuit in (a) are represented by an FID collection symbol at the corresponding points in the pulse sequence in (b).

We begin with the system in thermal equilibrium (and ignore the identity part of the density matrix, which does not evolve under rf pulses). The rf pulses $(\alpha)_j^i$ are written above each arrow, with α denoting the pulse flip angle, $i = 1,2$ denoting the qubit on which the pulse is being applied, and $j = x,y,z$ being the axis along which the pulse is applied. Spatial averaging (denoted by $Sp.Av.$) is achieved via a dephasing z gradient. The NMR spectra of the thermal state and the prepared NCC state are shown in Fig. 1(b), and the corresponding pulse sequence is depicted in Fig. 2(b). The quantum circuit to implement the nonclassicality witness map is shown in Fig. 2(a). The first module represents NCC state preparation using the pulses as already described. The circuit to capture nonclassicality of the prepared state consists of a controlled-Hadamard (CH) gate, followed by measurement on both qubits, a controlled-NOT (CNOT) gate, and finally, detection on "Qubit 2". The CH gate is analogous to a CNOT gate, with a Hadamard gate being implemented on the target qubit if the control qubit is in the state $|1\rangle$ and a "no operation" if the control qubit is in the state $|0\rangle$. The NMR pulse sequence corresponding to the quantum circuit is depicted in Fig. 2(b). The set of pulses grouped under the label "State prep". convert the thermal equilibrium state to the desired NCC state. A dephasing z gradient is applied on the gradient channel to kill undesired coherences. After a delay τ followed by the pulse sequence to implement the CH gate, the magnetizations of both qubits were measured with $\frac{\pi}{2}$ readout pulses (not shown in the figure). In the last part of the detection circuit a CNOT gate is applied followed by a magnetization measurement of "Qubit 2"; the scalar coupling time interval was set to $\tau_{12} = \frac{1}{4J}$, where J is the strength of the scalar coupling between the qubits. Refocusing pulses were used during all J evolution to compensate for unwanted chemical shift evolution during the selective pulses. State fidelity was computed using the Uhlmann-Jozsa measure [36,37], and the NCC state was prepared with a fidelity of 0.97 ± 0.02.

To detect the nonclassicality in the prepared NCC state via the map $\mathcal{W}_\sigma$, the expectation values of the operators $|00\rangle\langle 00|$ and $|1+\rangle\langle 1+|$ are required. Reworking the map brings it to the following form [25]:

$$\mathcal{W}_\sigma(\rho) = c_{\text{opt}} - \tfrac{1}{16}(1 + \langle Z_1\rangle + \langle Z_2\rangle + \langle Z_2'\rangle) \times (1 - \langle Z_1\rangle + \langle Z_2\rangle - \langle Z_2'\rangle),$$

where $\langle Z_1\rangle$ and $\langle Z_2\rangle$ are the magnetizations of "Qubit 1" and "Qubit 2" after a CH gate on the input state ρ, while $\langle Z_2'\rangle$ is the magnetization of "Qubit 2" after a CNOT gate. The

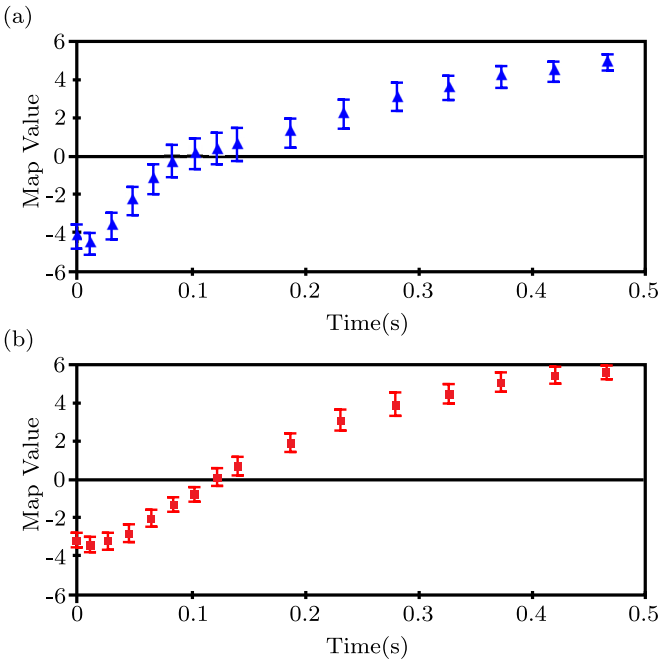

FIG. 3. (a) Experimental map value (in $\times 10^{-2}$ units) plotted as a function of time. (b) Map value (in $\times 10^{-2}$ units) directly calculated from the tomographically reconstructed state at each time instant.

theoretically expected normalized values of $\langle Z_1\rangle$, $\langle Z_2\rangle$, and $\langle Z_2'\rangle$ for state $\rho \equiv \sigma$ are 0, 1, and 0, respectively. The map value is $-0.067\,862 < 0$ and as desired, this map does indeed witness the presence of nonclassicality. The experimentally computed MV for the prepared NCC state turns out to be $-0.040\,6 \pm 0.005\,6$, proving that the map is indeed able to witness the nonclassicality present in the state.

C. Map value dynamics

The prepared NCC state was allowed to evolve freely in time and the MV calculated at each time instant in order to characterize the decoherence dynamics of the nonclassicality witness map. As theoretically expected, one should get a negative MV for states which are NCC. We measured MV at time instants which were integral multiples of $\frac{2}{J}$, i.e., $\frac{2n}{J}$ (with $n = 0, 1, 3, 5, 7, 9, 11, 13, 15, 20, 25, 30, 35, 40, 45,$ and 50), in order to avoid experimental errors due to J evolution. The results of experimental MV dynamics as a function of time are shown in Fig. 3(a). Experiments were repeated eight times to estimate the errors as depicted in the figure. As seen from Fig. 3(a), the MV remains negative (indicating the state is NCC) for up to 120 ms, which is approximately the ^{1}H transverse relaxation time. The standard NMR decoherence mechanisms are denoted by T_2, the spin-spin relaxation time, which causes dephasing among the energy eigenstates, and T_1, the spin-lattice relaxation time, which causes energy exchange between the spins and their environment. For comparison, the MV was also calculated directly using Eq. (6) with $c = c_{\text{opt}}$, from the state, which was tomographically reconstructed at each time instant via full state tomography [38]. The results are shown in Fig. 3(b), which are in good agreement with direct experimental MV measurements. The state fidelity was

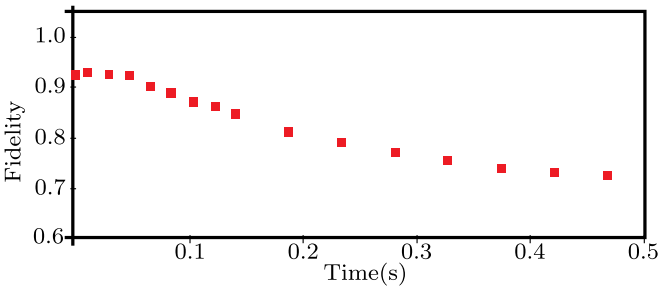

FIG. 4. Time evolution of state fidelity. The red squares represent fidelity of the experimentally prepared NCC state $\sigma_{\text{exp}}(t)$ evolving in time with regard to the theoretical NCC state at time $t = 0$.

also computed at the different time instants and the results are shown in Fig. 4. The red squares in Fig. 4 represent state fidelity of the experimental state $\sigma_{\text{exp}(t)}$ evolving in time with regard to the theoretical NCC state $\sigma_{\text{theo}}(0)$ at time $t = 0$ given in Eq. (3).

D. Quantum discord dynamics

We also compared the map value evaluation of nonclassicality with the standard measure of nonclassicality, namely, quantum discord [2,39]. The state was reconstructed by performing full quantum-state tomography and the quantum discord measure was computed from the experimental data. Quantum mutual information can be quantified by the equations

$$I(\rho_{AB}) = S(\rho_A) + S(\rho_B) - S(\rho_{AB}),$$
$$J_A(\rho_{AB}) = S(\rho_B) - S(\rho_B|\rho_A), \tag{7}$$

where $S(\rho_B|\rho_A)$ is the conditional von Neumann entropy of subsystem B when A has already been measured. Quantum discord is defined as the minimum difference between the two formulations of mutual information in Eq. (7):

$$D_A(\rho_{AB}) = S(\rho_A) - S(\rho_{AB}) + S\big(\rho_B\big|\big\{\Pi_j^A\big\}\big). \tag{8}$$

Quantum discord hence depends on projectors $\{\Pi_j^A\}$. The state of the system, after the outcome corresponding to projector $\{\Pi_j^A\}$ has been detected, is

$$\tilde{\rho}_{AB}\big|\big\{\Pi_j^A\big\} = \frac{\big(\Pi_j^A \otimes I_B\big)\rho_{AB}\big(\Pi_j^A \otimes I_B\big)}{p_j}, \tag{9}$$

with the probability $p_j = \text{Tr}[(\Pi_j^A \otimes I_B)\rho_{AB}(\Pi_j^A \otimes I_B)]$; I_B is an identity operator on subsystem B. The state of the system B, after this measurement, is

$$\rho_B\big|\big\{\Pi_j^A\big\} = \text{Tr}_A\big(\tilde{\rho}_{AB}\big|\big\{\Pi_j^A\big\}\big). \tag{10}$$

$S(\rho_B|\{\Pi_j^A\})$ is the missing information about B before measurement $\{\Pi_j^A\}$. The expression

$$S\big(\rho_B\big|\big\{\Pi_j^A\big\}\big) = \sum_j p_j S\big(\rho_B\big|\big\{\Pi_j^A\big\}\big) \tag{11}$$

is the conditional entropy appearing in Eq. (8). In order to capture the true quantumness of the correlation, one needs to perform an optimization over all sets of von Neumann–type measurements represented by the projectors $\{\Pi_j^A\}$. We define

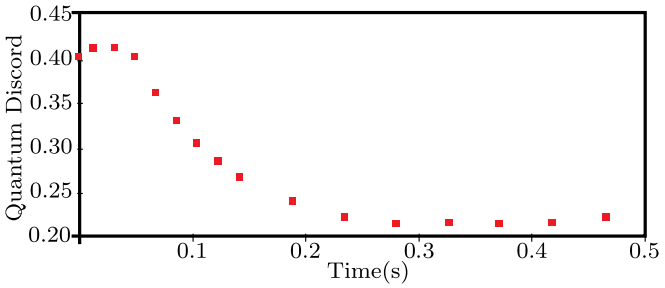

FIG. 5. Time evolution of quantum discord (characterizing total quantum correlations present in the state) for the NCC state.

two orthogonal vectors (for spin half quantum subsystems), characterized by two real parameters θ and ϕ, on the Bloch sphere as follows:

$$\cos\theta|0\rangle + e^{\iota\phi}\sin\theta|1\rangle,$$
$$e^{-\iota\phi}\sin\theta|0\rangle - \cos\theta|1\rangle. \quad (12)$$

These vectors can be used to construct the projectors $\Pi_{1,2}^{A,B}$, which are then used to find the state of B after an arbitrary measurement was made on subsystem A. The definition of conditional entropy [Eq. (11)] can be used to obtain an expression which is parameterized by θ and ϕ for a given state ρ_{AB}. This expression is finally minimized by varying θ and ϕ and feeding the results back into Eq. (8), which yields a measure of quantum discord independent of the basis chosen for the measurement of the subsystem.

To compare the detection via the positive map method with the standard quantum discord measure, we let the state evolve for a time τ and then reconstructed the experimentally prepared via full quantum-state tomography and calculated the quantum discord at all time instants where the MV was determined experimentally (the results are shown in Fig. 5). At $\tau = 0$ s, a nonzero quantum discord confirms the presence of NCC and verifies the results given by MV. As the state evolves with time, the quantum discord parameter starts decreasing rapidly, in accordance with increasing MV. Beyond 120 ms, while the MV becomes positive and hence fails to detect nonclassicality, the discord parameter remains nonzero, indicating the presence of some amount of nonclassicality (although by this time the state fidelity has decreased to 0.7). However, value of quantum discord is very close to zero and in fact cannot be distinguished from contributions due to noise. One can hence conclude that the positive map suffices to detect nonclassicality when decoherence processes have not set in and while the fidelity of the prepared state is good. Once the state has decohered, however, a measure such as quantum discord has to be used to verify whether the degraded state retains some amount of nonclassical correlations or not. While the constructed nonclassicality witness is not optimal and hence cannot be quantitatively compared with a stricter measure of nonclassicality, such as a measurement of the quantum discord parameter, in most cases the witness suffices to detect the presence of nonclassicality in a quantum state without having to resort to more complicated experimental schemes.

III. CONCLUSIONS

In this work we experimentally detected nonclassical correlations in a separable two-qubit quantum state using a nonlinear positive map as a nonclassicality witness. The witness is able to detect nonclassicality, and its obvious advantage lies in its using much fewer experimental resources as compared to quantifying nonclassicality by measuring discord via full quantum-state tomography. It will be interesting to construct and utilize this map in higher-dimensional quantum systems and for greater than two qubits, where it is more difficult to distinguish between classical and quantum correlations.

It has been posited that quantum correlations captured by quantum discord which go to quantum entanglement and can thus be present even in separable states are responsible for achieving computational speedup in quantum algorithms. It is hence important, from the point of view of quantum information processing, to confirm the presence of such correlations in a quantum state, without having to expend too much experimental effort, and our work is a step forward in this direction.

ACKNOWLEDGMENTS

All experiments were performed on a Bruker Avance-III 600-MHz FT-NMR spectrometer at the NMR Research Facility at IISER Mohali. A. acknowledges funding from DST India under Grant No. EMR/2014/000297. K.D. acknowledges funding from DST India under Grant No. EMR/2015/000556.

[1] M. A. Nielsen and I. L. Chuang, *Quantum Computation and Quantum Information* (Cambridge University Press, Cambridge, UK, 2000).
[2] H. Ollivier and W. H. Zurek, Phys. Rev. Lett. **88**, 017901 (2001).
[3] K. Modi, A. Brodutch, H. Cable, T. Paterek, and V. Vedral, Rev. Mod. Phys. **84**, 1655 (2012).
[4] A. Ferraro, L. Aolita, D. Cavalcanti, F. M. Cucchietti, and A. Acín, Phys. Rev. A **81**, 052318 (2010).
[5] K. Bartkiewicz, K. Lemr, A. Černoch, and J. Soubusta, Phys. Rev. A **87**, 062102 (2013).
[6] D. O. Soares-Pinto, L. C. Céleri, R. Auccaise, F. F. Fanchini, E. R. deAzevedo, J. Maziero, T. J. Bonagamba, and R. M. Serra, Phys. Rev. A **81**, 062118 (2010).
[7] J. Maziero, R. Auccaise, L. C. Céleri, D. O. Soares-Pinto, E. R. deAzevedo, T. J. Bonagamba, R. S. Sarthour, I. S. Oliveira, and R. M. Serra, Braz. J. Phys. **43**, 86 (2013).
[8] G. Passante, O. Moussa, D. A. Trottier, and R. Laflamme, Phys. Rev. A **84**, 044302 (2011).
[9] R. Auccaise, L. C. Céleri, D. O. Soares-Pinto, E. R. deAzevedo, J. Maziero, A. M. Souza, T. J. Bonagamba, R. S. Sarthour, I. S. Oliveira, and R. M. Serra, Phys. Rev. Lett. **107**, 140403 (2011).
[10] H. Singh, Arvind, and K. Dorai, arXiv:1610.02755v1.
[11] A. Datta, S. T. Flammia, and C. M. Caves, Phys. Rev. A **72**, 042316 (2005).
[12] A. F. Fahmy, R. Marx, W. Bermel, and S. J. Glaser, Phys. Rev. A **78**, 022317 (2008).

[13] B. Eastin, New J. Phys. **18**, 021003 (2016).
[14] Y. Huang, New J. Phys. **16**, 033027 (2014).
[15] H. Cable and D. E. Browne, New J. Phys. **17**, 113049 (2015).
[16] A. SaiToh, R. Rahimi, and M. Nakahara, Quantum Inf. Process. **10**, 431 (2011).
[17] R. Rahimi, K. Takeda, M. Ozawa, and M. Kitagawa, J. Phys. A: Math. Gen. **39**, 2151 (2006).
[18] R. Rahimi, A. SaiToh, M. Nakahara, and M. Kitagawa, Phys. Rev. A **75**, 032317 (2007).
[19] J. G. Filgueiras, T. O. Maciel, R. E. Auccaise, R. O. Vianna, R. S. Sarthour, and I. S. Oliveira, Quantum Inf. Process. **11**, 1883 (2011).
[20] J. Maziero and R. M. Serra, Int. J. Quantum Inform. **10**, 1250028 (2012).
[21] R. Auccaise, J. Maziero, L. C. Céleri, D. O. Soares-Pinto, E. R. deAzevedo, T. J. Bonagamba, R. S. Sarthour, I. S. Oliveira, and R. M. Serra, Phys. Rev. Lett. **107**, 070501 (2011).
[22] D. O. Soares-Pinto, R. Auccaise, J. Maziero, A. Gavini-Viana, R. M. Serra, and L. C. Céleri, Philos. Trans. R. Soc. A **370**, 4821 (2012).
[23] G. H. Aguilar, O. Jiménez Farías, J. Maziero, R. M. Serra, P. H. S. Ribeiro, and S. P. Walborn, Phys. Rev. Lett. **108**, 063601 (2012).
[24] A. SaiToh, R. Rahimi, and M. Nakahara, Phys. Rev. A **77**, 052101 (2008).
[25] R. Rahimi and A. SaiToh, Phys. Rev. A **82**, 022314 (2010).
[26] J. Du, N. Xu, X. Peng, P. Wang, S. Wu, and D. Lu, Phys. Rev. Lett. **104**, 030502 (2010).
[27] J. Pearson, G. Feng, C. Zheng, and G. Long, Sci. China: Phys., Mech. Astron. **59**, 120312 (2016).
[28] I. A. Silva, A. M. Souza, T. R. Bromley, M. Cianciaruso, R. Marx, R. S. Sarthour, I. S. Oliveira, R. Lo Franco, S. J. Glaser, E. R. deAzevedo, D. O. Soares-Pinto, and G. Adesso, Phys. Rev. Lett. **117**, 160402 (2016).
[29] I. A. Silva, D. Girolami, R. Auccaise, R. S. Sarthour, I. S. Oliveira, T. J. Bonagamba, E. R. deAzevedo, D. O. Soares-Pinto, and G. Adesso, Phys. Rev. Lett. **110**, 140501 (2013).
[30] O. Guhne and G. Toth, Phys. Rep. **474**, 1 (2009).
[31] J. Oppenheim, M. Horodecki, P. Horodecki, and R. Horodecki, Phys. Rev. Lett. **89**, 180402 (2002).
[32] A. Peres, Phys. Rev. Lett. **77**, 1413 (1996).
[33] R. Horodecki, P. Horodecki, M. Horodecki, and K. Horodecki, Rev. Mod. Phys. **81**, 865 (2009).
[34] V. Vedral, Found. Phys. **40**, 1141 (2010).
[35] A. Streltsov, H. Kampermann, and D. Bruß, Phys. Rev. Lett. **107**, 170502 (2011).
[36] A. Uhlmann, Rep. Math. Phys. **9**, 273 (1976).
[37] R. Jozsa, J. Mod. Opt. **41**, 2315 (1994).
[38] G. M. Leskowitz and L. J. Mueller, Phys. Rev. A **69**, 052302 (2004).
[39] S. Luo, Phys. Rev. A **77**, 042303 (2008).